Available online at www.sciencedirect.com

SCIENCE DIRECT®

Journal of Catalysis 220 (2003) 66–73

JOURNAL OF CATALYSIS

www.elsevier.com/locate/jcat

High-pressure liquid phase hydroconversion of heptane/nonane mixtures on Pt/H-Y zeolite catalyst

Joeri F.M. Denayer,[a,*] Refik A. Ocakoglu,[a] Ward Huybrechts,[b] Bruno Dejonckheere,[b] Pierre Jacobs,[b] Sofia Calero,[c] Rajamani Krishna,[c] Berend Smit,[c] Gino V. Baron,[a] and Johan A. Martens [b]

[a] *Dienst Chemische Ingenieurstechniek, Vrije Universiteit Brussel, Pleinlaan 2, B-1050 Brussel, Belgium*
[b] *Centrum voor Oppervlaktechemie en Katalyse, Katholieke Universiteit Leuven, Kasteelpark Arenberg 23, B-3001 Leuven, Belgium*
[c] *Department of Chemical Engineering, University of Amsterdam, Nieuwe Achtergracht 166, 1018 WV Amsterdam, The Netherlands*

Received 3 February 2003; revised 16 May 2003; accepted 16 May 2003

Abstract

The competitive hydroconversion of heptane and nonane molecules in their mixture was studied in a continuous flow, fixed-bed reactor filled with Pt/HY zeolite catalyst. Liquid-phase reaction conditions were established at reaction temperatures of 230, 250, and 270 °C by pressurizing the reactor at 100 bar. Hydrogen was supplied in an absorbed state with the liquid hydrocarbon feed. Under these liquid-phase reaction conditions, the apparent reaction rates of heptane and nonane were almost identical. In a similar experiment under vapor-phase conditions, nonane was much more reactive than heptane. The conversion data under liquid-phase conditions were analyzed with an adsorption-reaction model based on intrinsic kinetic parameters obtained from vapor-phase experiments. The model revealed that the enhanced reactivity of heptane in the liquid phase was due to its preferential adsorption. Simulation of the adsorption of the heptane/nonane mixture in the pores of zeolite Y with the configurational-bias Monte Carlo method confirmed the preferential adsorption of heptane in zeolite Y at high pressure. Under such conditions, in zeolite Y supercages the packing of the smaller heptane molecules is more favorable than that of the larger nonane molecules.

Keywords: Hydrocracking; Alkane mixtures; Molecular competition; Pt/HY zeolite; Liquid phase; High pressure; CBMC simulation

1. Introduction

In petroleum refinery, governing the relative reactivity of the different hydrocarbon molecules is of prime importance. For example, in alkane isomerization processes for octane boosting, it is desirable to isomerize simultaneously the C5, C6, C7, and C8 fractions. In the current zeolite catalyst-based vapor-phase processes, the C8 and C7 alkanes are much too reactive compared to C5 and C6. This is because in the vapor phase, there is preferential physisorption of long alkanes over short alkanes, resulting in higher concentrations of the larger molecules at the active sites [1,2]. Long alkanes are then converted preferentially from their mixtures with shorter alkanes. In the hysomer process [3], the mixture of C5 and C6 straight alkane molecules is branched using bifunctional mordenite catalysts. In the present processes, extending the feed fraction to include C7 and C8 *n*-alkanes is not possible, since at reaction severity needed to convert C5 and C6, there is a too high conversion of C7 and C8 giving rise to undesired cracking of these molecules into gaseous compounds.

For experimental reasons, academic studies on isomerization and hydrocracking, or in short hydroconversion, are usually performed using a hydrocarbon vapor and a hydrogen pressure below 10 bar. Such reaction conditions are suitable for studying hydroconversions of model alkanes and to disentangle the underlying reaction mechanisms and kinetics [4–14]. Recently, some of us reported that in hydroconversions of alkane mixtures on Pt/US-Y zeolite, the molecular competitions in the liquid phase are very different from those in the vapor phase [15]. Short and long alkanes adsorb in a nonselective way in US-Y-type zeolites under liquid phase conditions [16]. The mesopores that are present

* Corresponding author.
E-mail address: Joeri.Denayer@vub.ac.be (J.F.M. Denayer).

0021-9517/$ – see front matter
doi:10.1016/S0021-9517(03)00239-2

in Pt/H-USY zeolite crystals do not impose any steric constraints on the adsorbing molecules. Thus, the composition of the bulk liquid is established inside the zeolite and apparent reaction rates correspond to intrinsic reaction kinetics [15].

Theoretical calculations by Talbot [17] and Smit and coworkers [18–20] revealed that in mixtures of molecules of different molecular size, the adsorption selectivity for the smallest molecule increases with increasing degree of micropore filling. A reversal of the adsorption selectivity might even occur under conditions near to complete saturation of the pores. Such a reversal effect occurs because in a confined environment small molecules can more efficiently be packed compared to large molecules.

In the present work, we verified experimentally whether such reversal of the adsorption selectivity can be exploited in a catalytic process. For experimental reasons, the combination of heptane and nonane was selected. With these molecules, a pressure of 100 bar is sufficient to achieve liquid-phase conditions at temperatures of 230–270 °C. The catalyst of choice was Pt/H-Y zeolite devoid of mesopores. Mesopores in the Y zeolite had to be avoided, since in these wide pores there is no reversal of adsorption selectivity. The adsorption selectivity was derived from the catalytic conversion data using an adsorption-reaction model. Configurational-bias Monte Carlo simulations of the adsorption of mixtures of heptane and nonane were performed to complement the results of the catalytic reaction modeling.

2. Experimental

2.1. Catalytic experiments

The H-Y zeolite (CBV500, Si/Al 2.6, Zeolyst) was loaded with 0.5 wt% platinum by incipient wetness impregnation with aqueous $Pt(NH_3)_4Cl_2$ solution. The zeolite powder was compressed into a solid disk, crushed, and sieved into 125- to 250- and 250- to 500-μm pellet fractions for filling the reactor tubes. The catalyst activation procedure comprised calcination under flowing oxygen at 400 °C followed by reduction in hydrogen at the same temperature.

Vapor-phase catalytic experiments with heptane and nonane individually were performed in a high-throughput 15 parallel reactor equipment with on-line product analysis with multicapillary GC [21]. These experiments were performed on 35-mg catalyst pellets of 125–250 μm at 230, 250, and 270 °C, at a total pressure of 4.5 bar, and hydrocarbon partial pressures of 0.003, 0.1, and 0.3 bar.

The conversion of an equimolar mixture of heptane and nonane was done in a conventional fixed-bed reactor filled with 210 mg of 250 to 500-μm pellets, equipped with a liquid feed delivery pump and vaporization chamber. The total hydrocarbon pressure was 0.3 bar, the total reactor pressure 4.5 bar, and the temperature 230, 250, or 270 °C. Analysis of the reaction products was done on-line using capillary GC, splitless cool-on-column injection, and temperature programming from 10 to 114 °C.

Liquid-phase catalytic experiments were performed in a tubular reactor with an equimolar mixture of heptane and nonane at a total reactor pressure of 100 bar, reactor temperatures of 230, 250, and 270 °C, and a H_2/hydrocarbon molar ratio of 0.5. Samples of the reactor effluent were analyzed on-line by capillary GC using a four-way sampling valve with small internal sample volume of 1 μL and using the same temperature programming as in the vapor-phase experiments with the conventional reactor. A more detailed description of the experimental procedure is given elsewhere [14].

2.2. Adsorption parameters

Vapor-phase adsorption isotherms of heptane and nonane on the CBV500 Y-type zeolite used here were determined in previous work by perturbation chromatography, and published elsewhere [22]. These isotherms can be represented by a Langmuir expression over the experimental hydrocarbon pressure range of the vapor-phase experiments (0–0.3 bar),

$$q_i(p,T) = \frac{K_i' p_i}{1 + \sum_j L_j p_j}, \tag{1}$$

where q_i is adsorbed amount of component i; K_i' its Henry constant; p_i its partial pressure, and L_i its Langmuir constant. The experimental Henry constants K_i' of heptane and nonane at 230, 250, and 270 °C are given in Table 1. This table also reports the saturation capacities $q_{\mathrm{sat},i}$ of the zeolite for both components, calculated using the theoretical zeolite Y crystal structure and using the theoretical liquid density at 100 bar (calculated using a Peng–Robinson with a modified equation of state as available in ASPEN).

2.3. Reaction model

Adsorbed alkanes are dehydrogenated on the platinum clusters in the zeolite pores. The resulting alkenes are protonated and isomerized on the Brønsted acid sites of the zeolite. The concentration of alkenes q_O is related to the alkane concentration q_A via the hydrogenation/dehydrogenation equilibrium, which for the vapor-phase experiments corresponds to

$$q_O = \frac{K_{DH}^{vap} q_A}{p_{H_2}}, \tag{2}$$

in which K_{DH}^{vap} represents the dehydrogenation constant in vapor phase and p_{H_2} the hydrogen partial pressure. For the liquid-phase conditions, the following equation applies [23],

$$q_O = \frac{K_{DH}^{vap} q_A}{C_{H_2}^L \phi_{H_2}^L P V_m}, \tag{3}$$

Table 1
Model parameters (experimental Henry adsorption constants, theoretical saturation capacities, and lumped kinetic constants ($k_L = K_{DH}k_{intr}$) of heptane and nonane)

	Kinetic parameters	Adsorption parameters					
		C9			C7		
	k_L (bar/s) C9/C7	K' (mol/(kg bar))	q_{sat}[a] (mol/kg)	q_{sat}[a] (molecules/supercage)	K' (mol/(kg bar))	q_{sat}[a] (mol/kg)	q_{sat}[a] (molecules/supercage)
230 °C	0.11/0.06	151.0	1.29	1.86	21.5	1.51	2.17
250 °C	0.31/0.22	93.5	1.25	1.80	14.6	1.43	2.06
270 °C	0.70/0.55	55.5	1.20	1.73	9.5	1.34	1.93

[a] Calculated using theoretical crystal structure and theoretical liquid density at 100 bar.

where $C^L_{H_2}$ stands for the dissolved hydrogen concentration, $\phi^L_{H_2}$ represents the fugacity coefficient of hydrogen in the liquid phase, and V_m equals the molar volume of the liquid phase and P the total pressure.

The catalytic conversion of heptane and nonane can be represented by the following classical kinetic model (5):

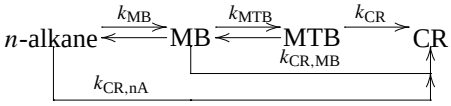

(4)

According to this reaction scheme, n-alkanes are first isomerized into monobranched alkanes (MB). Subsequent isomerization reactions lead to the formation of isomers with multibranched skeletons (MTB), which are easily cracked into shorter alkane fragments (CR). Formation of short alkanes is also possible via cracking of monobranched and linear alkanes, depending on the reaction conditions. The following rate equations hold for this reaction scheme:

$$r_{nA,i} = k_{MB,i}\left(q_{nO,i} - \frac{q_{MBO,i}}{K_{MB,i}}\right) - k_{CR,nO}q_{nO,i}, \tag{5}$$

$$r_{MB,i} = \left(k_{MB,i}\left(q_{nO,i} - \frac{q_{MBO,i}}{K_{MB,i}}\right) - k_{MTB,i}\left(q_{MB,i} - \frac{q_{MTBO,i}}{K_{MTB,i}}\right) - k_{CR,MBO,i}q_{MBO,i}\right), \tag{6}$$

$$r_{MTB,i} = k_{MTB,i}\left(q_{MBO,i} - \frac{q_{MTBO,i}}{K_{MTB,i}}\right) - k_{CR,i}q_{MTBO,i}, \tag{7}$$

$$r_{CR,i} = k_{CR,i}q_{MTBO,i} + k_{CR,nO,i}q_{nO,i} + k_{CR,MBO,i}q_{MBO,i}. \tag{8}$$

K_{MB} and K_{MTB} represent the equilibrium constant between linear and monobranched, and monobranched and multibranched alkanes, respectively.

The vapor-phase, single component conversion data at the three experimental temperatures, and the three HC/H_2 ratios, were fitted to rate Eqs. (5)–(8). The experimentally determined adsorption parameters (Eq. (1) and Table 1) were used in these calculations. The sum of $K_{DH} * k_{MB}$ and $K_{DH} * k_{CR,nA}$ for both components at 230, 250, and 270 °C was combined into kinetic constants $k_{L,i}$ (Table 1), which were used further on in the analysis of the conversions of the mixtures in vapor and liquid phase.

2.4. Configurational-bias Monte Carlo simulations

Adsorption isotherms were computed using configurational-bias Monte Carlo (CBMC) simulations in the grand-canonical ensemble, where the temperature and chemical potentials are imposed [24]. Instead of inserting a molecule at a random position, in a CBMC simulation a molecule is grown atom by atom in such a way that the "empty spots" in the zeolite are found. This growing scheme gives a bias that is removed exactly by adjusting the acceptance rules [25]. Simulations were carried out in cycles and in each cycle, an attempt to perform one of the following moves was made: (1) displacement of a randomly selected chain, (2) rotation of a chain around its center of mass, (3) partly regrowing of a chain, (4) exchange with a reservoir, and (5) change of identity.

The relative probabilities for attempting these moves were 15% displacements, 15% rotations, 15% partial regrowths, and 50% exchanges with the reservoir, and the remaining 5% of the moves were attempts to change the identity of a molecule. The number of trial orientations in the configurational-bias Monte Carlo scheme was six for all molecules. In addition, we used the multiple first bead scheme with 15 trial positions for the first bead [26].

The alkanes were described with a united atom model, in which each CH_n group is treated as a single interaction center [27]. The interactions between these pseudo-atoms are given by Lennard-Jones potentials. The interactions of the adsorbed molecules with the zeolite are dominated by the dispersive forces between the pseudo-atoms and the oxygen atoms of the zeolite [28,29] meaning that the silicon interactions are taken into account through an effective potential with only the oxygens. The nonframework sodium cations are also described as single charged interaction centers where the interactions of cations with other adsorbates and the zeolite are modeled by Lennard-Jones and Coulombic interactions. The NaY zeolite lattice [30] is considered rigid during the simulations but the nonframework sodium cations are allowed to move. More detailed information of our models and simulation methods are given elsewhere [31,32].

3. Results

3.1. Pure components, vapor phase

The conversion of heptane and nonane in separate experiments at hydrocarbon partial pressures of 0.003, 0.1, and 0.3 bar as a function of the space time at 230 °C is shown in Fig. 1. In all graphs, the solid curves represent the model values, obtained by fitting of the experimental data. At the lowest pressure (0.003 bar), the difference in reactivity between nonane and heptane is most pronounced. At low pressures, the concentration of adsorbed molecules is a linear function of the Henry adsorption constant. Hence the concentration of nonane molecules in the zeolite pores is much larger than heptane as a result of its much higher Henry constant (Table 1). With increasing pressure, the pores become more filled and finally reach saturation from a certain pressure onward. In the plateau region of the adsorption isotherm, the relative amounts adsorbed no longer reflect the Henry adsorption constants, but rather the saturation capacity for both components, explaining the much smaller difference in apparent reactivity at the hydrocarbon partial pressure of 0.3 bar. Although a broad range of reactivities is observed in the present experiments, the use of an adequate adsorption expression allowed a fit of the kinetic data with one parameter set (Table 1, Fig. 1). The temperature dependence of the nonane and heptane conversion on Pt/H-Y and the excellent agreement of experimental data with the model is shown in Fig. 2.

3.2. Equimolar mixture, vapor phase

The conversion of an equimolar heptane/nonane mixture at a hydrocarbon partial pressure of 0.3 bar and a total reactor pressure of 4.5 bar at 230, 250, and 270 °C is shown in Fig. 3. At all reaction temperatures, nonane is converted much faster than heptane. For example, the ratio of initial reaction rates of nonane and heptane at 230 °C equals 6 for the mixture, while a ratio of less than 2 is observed for the pure components at hydrocarbon partial pressures of 0.1 and 0.3 bar (Fig. 1). These observations are in line with previous work and are explained by a selective adsorption of the heaviest compound, nonane, from the mixture in vapor phase.

3.3. Equimolar mixture, liquid phase

In Fig. 4, the conversion of nonane and heptane is shown as a function of the average mixture conversion for the liquid- and vapor-phase conditions at 250 °C. In liquid phase at 100 bar, the conversion rate of nonane is only slightly higher than that of heptane, and the competition effects between both components are significantly lower compared to the vapor phase. In Fig. 5, the conversion of heptane is plotted as a function of the nonane conversion for the liquid-phase conditions at 230, 250, and 270 °C. At 230 and

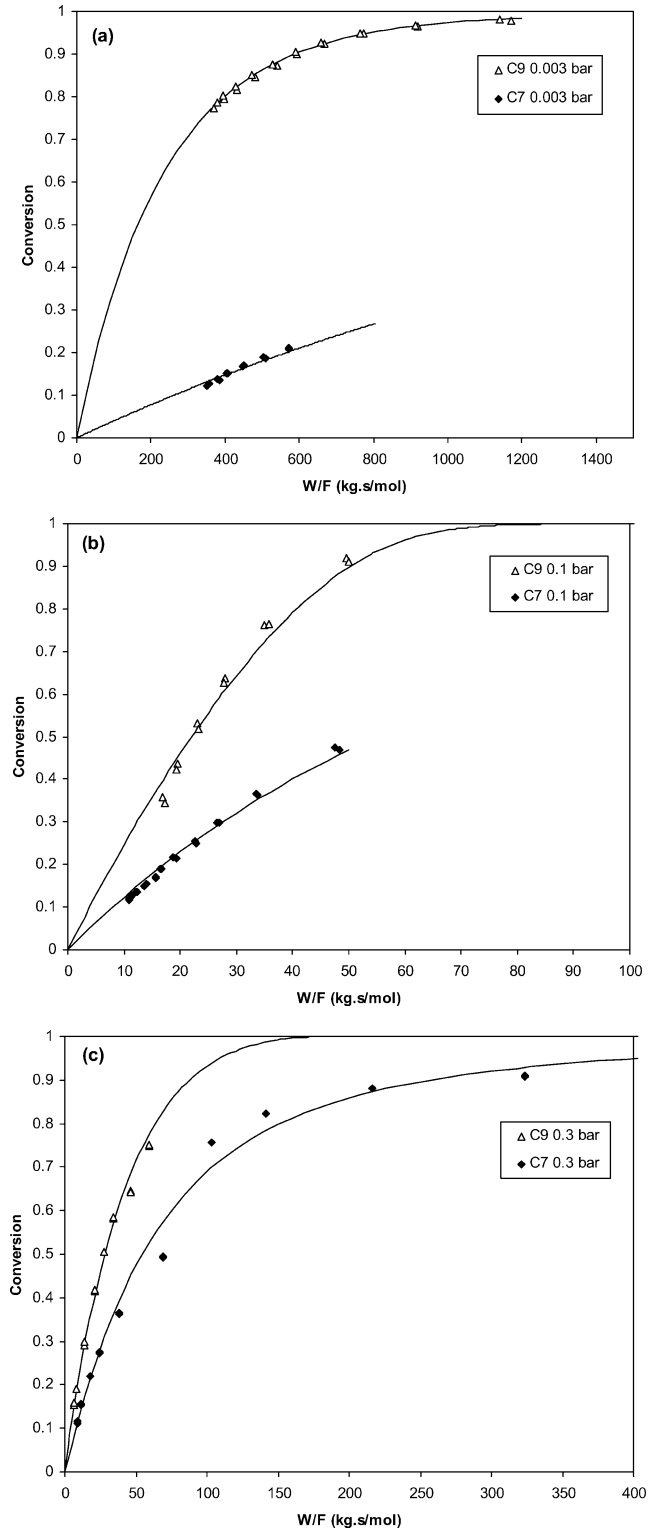

Fig. 1. Conversion of pure nonane and heptane on Pt/HY at 230 °C: (a) $P_{HC} = 0.003$ bar, $P_T = 4.5$ bar, (b) $P_{HC} = 0.1$ bar, $P_T = 4.5$ bar, (c) $P_{HC} = 0.3$ bar, $P_T = 4.5$ bar.

250 °C, the experimental data points almost fall onto the bisecting line, while a small preference for nonane conversion is observed at 270 °C. In the same graph, previously obtained data on the liquid- and vapor-phase conversion of an

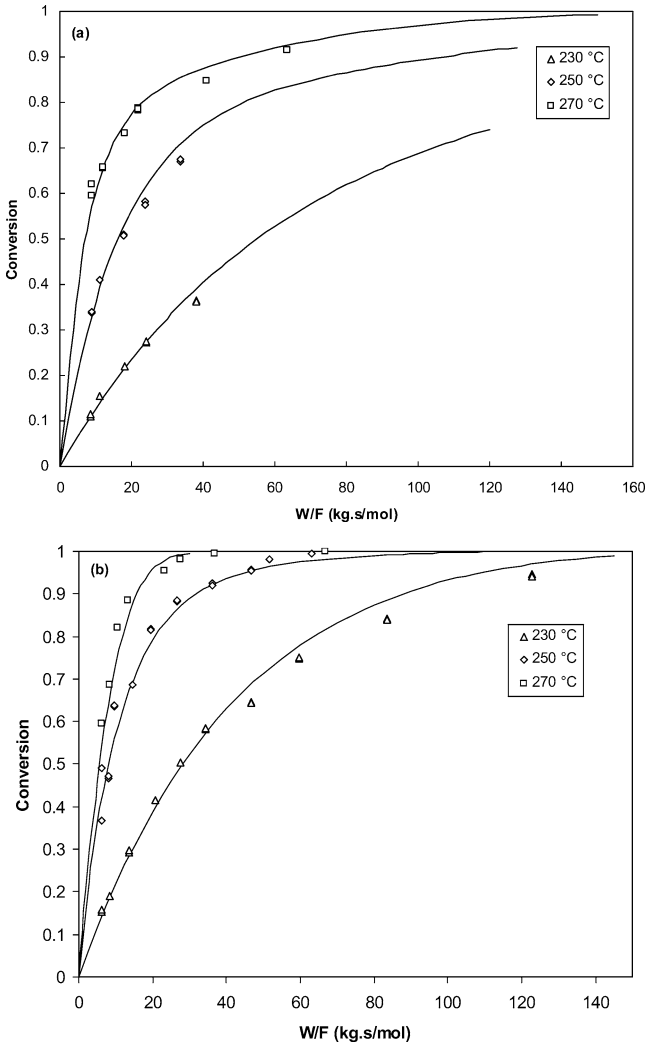

Fig. 2. (a) Heptane and (b) nonane conversion at 230, 250, and 270 °C ($P_{HC} = 0.3$ bar, $P_T = 4.5$ bar).

equimolar heptane/nonane mixture on a Pt/H-USY catalyst are added for comparison [12]. Although both catalysts behave similarly in the vapor phase, the differences in observed reactivity under high-pressure liquid-phase conditions are much smaller on Pt/H-Y compared to Pt/H-USY.

Since no experimental data on the binary adsorption of heptane and nonane in liquid phase are available, the amounts adsorbed in liquid phase were estimated by fitting the experimental catalytic data to the model [Eqs. (1), (3), (5)–(8)], using the intrinsic kinetic parameters obtained from the pure component experiments and leaving the amounts adsorbed q_i as fitting parameters (Table 1).

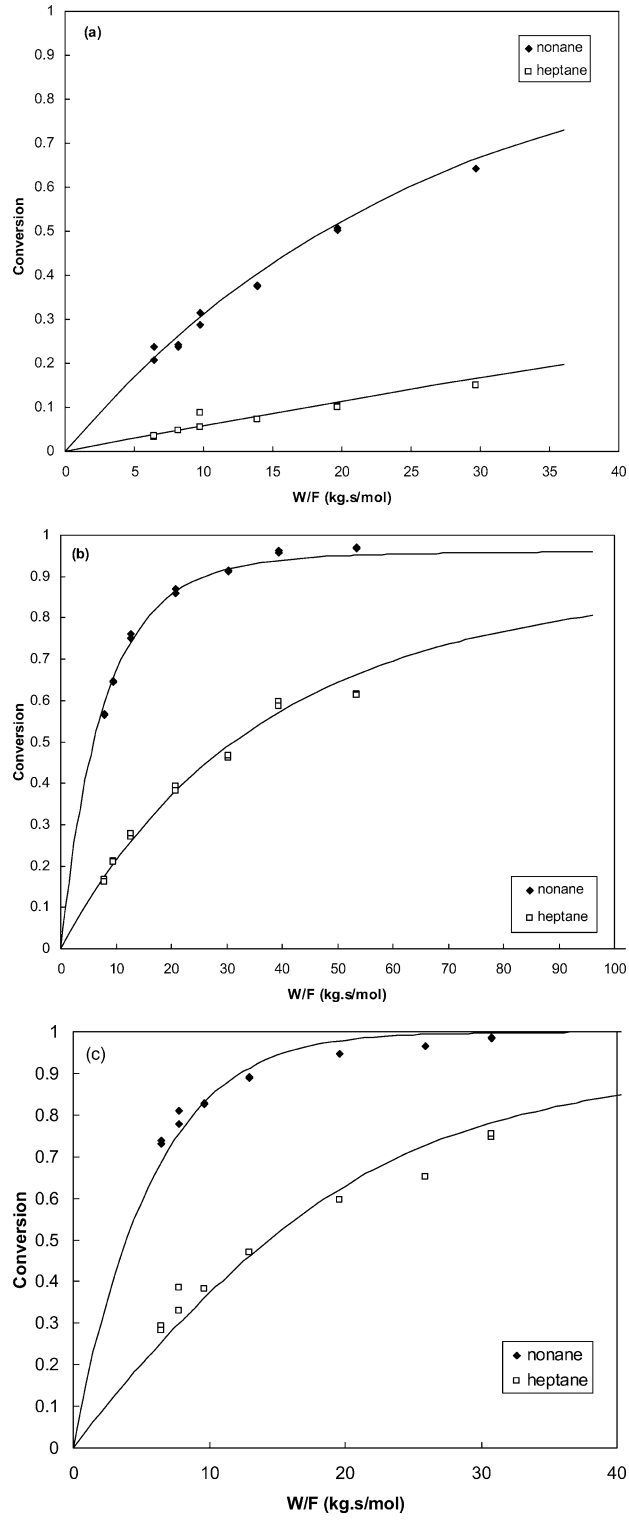

Fig. 3. Conversion of nonane and heptane from their equimolar mixture on Pt/HY at (a) 230 °C, (b) 250 °C, (c) 270 °C ($P_{HC} = 0.32$ bar, $P_T = 4.5$ bar).

4. Discussion

As observed previously with a Pt/H-USY catalyst [14], the differences in observed reactivity between short and long alkanes in the hydroconversion of alkane mixtures are smaller in the liquid phase compared to the vapor phase. In the mesopores of Pt/H-USY, alkanes of different chain length are adsorbed in a nonselective way from a liquid phase. Hence the ratio of relative reactivities in the liquid phase corresponds to the ratio of intrinsic kinetic constants

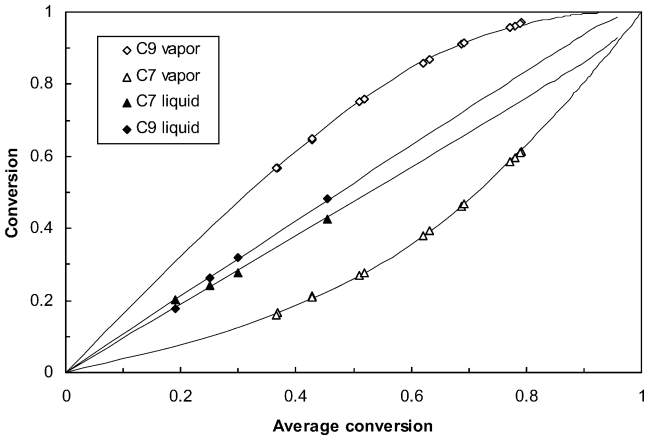

Fig. 4. Conversion of nonane and heptane as a function of the average mixture conversion on Pt/HY in vapor and liquid phases at 250 °C.

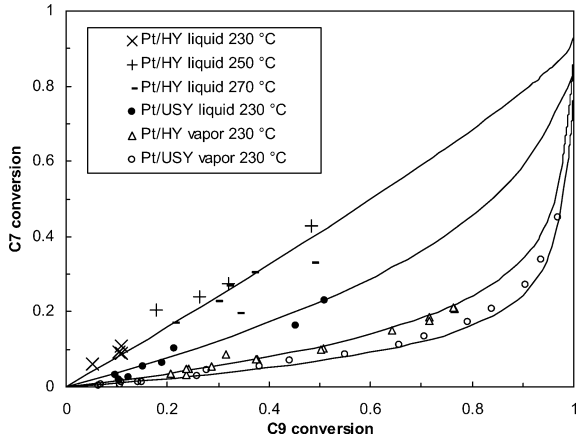

Fig. 5. Heptane conversion as a function of the nonane conversion in liquid and vapor phases on Pt/HY and Pt/H-USY.

on Pt/H-USY. On Pt/H-Y, the differences in observed reaction rate between nonane and heptane in the liquid phase are smaller than would be expected from the intrinsic kinetics (Table 1). It appears that the difference in intrinsic reactivity in favor of nonane is balanced by preferential adsorption of heptane. Unfortunately, experimental liquid-phase adsorption data at high temperatures and 100 bar pressure are not available.

Since the kinetic constants of heptane and nonane are known from the pure component experiments, the amounts adsorbed in the liquid-phase catalytic experiments can be calculated by fitting of the rate equations to the experimental conversion data, leaving the amounts adsorbed as parameters to be estimated. The ratio of adsorbed amounts calculated in this manner is given in Table 2. At 230 and 250 °C, the amount of nonane in the pores is respectively only 0.6 and 0.8 times the adsorbed heptane concentration, confirming a preferential adsorption of heptane. At 270 °C, the adsorbed nonane concentration is 1.4 times the adsorbed heptane concentration, which is still a much smaller ratio than expected on the basis of the ratio of Henry adsorption constants, viz. 5.8 (Table 2).

Table 2
Relative amounts adsorbed of nonane and heptane at zero coverage and at 100 bar

	$q_{0\,C9}/q_{0\,C7}$	$q_{C9\,100\ bar}/q_{C7\,100\ bar}$
230 °C	7.0	0.6
250 °C	6.4	0.8
270 °C	5.8	1.4

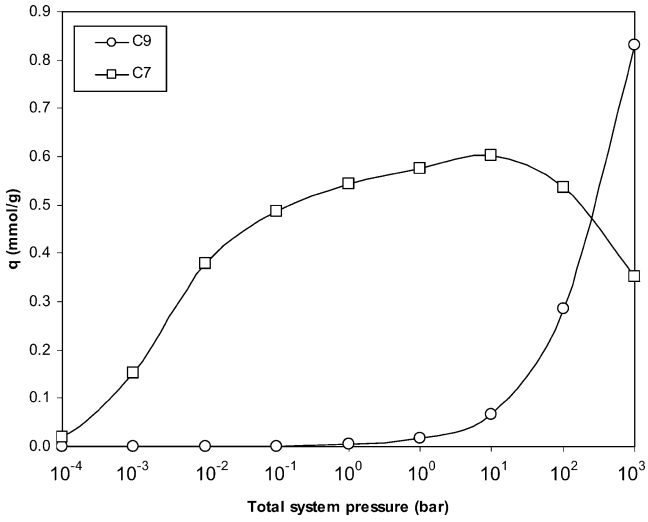

Fig. 6. Adsorption of an equimolar heptane/nonane mixture on NaY at 230 °C as a function of the total pressure as calculated by configurational-bias Monte Carlo simulations.

Our simulation results for the adsorption of an equimolar heptane/nonane mixture are shown in Fig. 6. This graph represents the amounts adsorbed of nonane and heptane from their equimolar mixture on a NaY zeolite as a function of the total mixture pressure as calculated by configurational-bias Monte Carlo simulations. At low pressures, nonane is selectively adsorbed in the pores of the NaY zeolite. From a pressure of 10 bar on, the amount adsorbed of nonane starts to decrease, and nonane molecules are replaced by the smaller heptane molecules. At a pressure of 300–400 bar, both components adsorb to the same extent, and at 1000 bar, the amount of heptane adsorbed has become 2.4 times larger than the amount of nonane adsorbed.

Although the theoretical absolute pressure (> 300 bar) at which reversal of adsorption selectivity occurs is higher than the experimental pressure at which inversion was observed (100 bar), the simulations clearly demonstrate the effect of pressure on molecular competition. Differences between our experiments and simulations are mainly due to the fact that during the simulations we are considering “ideal” crystals with a bigger pore volume. For this reason higher pressures are necessary to reach the saturation loadings and also to observe the inversion in the selectivity.

Besides, under catalytic conditions the pores of the zeolite contain not only heptane and nonane but also dissolved hydrogen, alkane isomers, and light products from cracking,

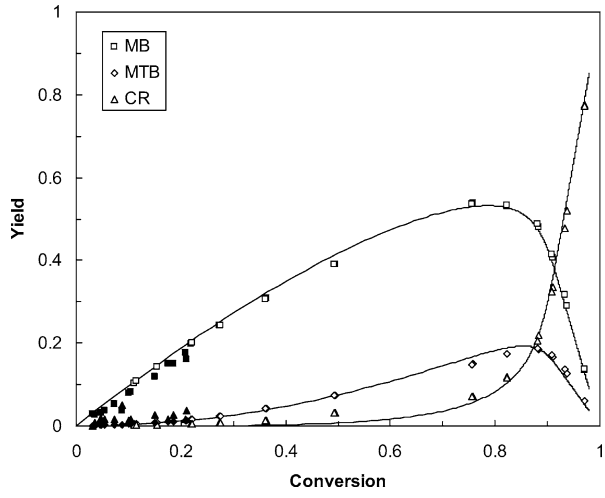

Fig. 7. Yield of monobranched, multibranched, and cracked alkanes in the hydroconversion of heptane on Pt/H-Y at 230 °C as a function of the total conversion (open symbols, pure heptane in the vapor phase; closed symbols, heptane in mixture with nonane in the vapor phase; lines, model values).

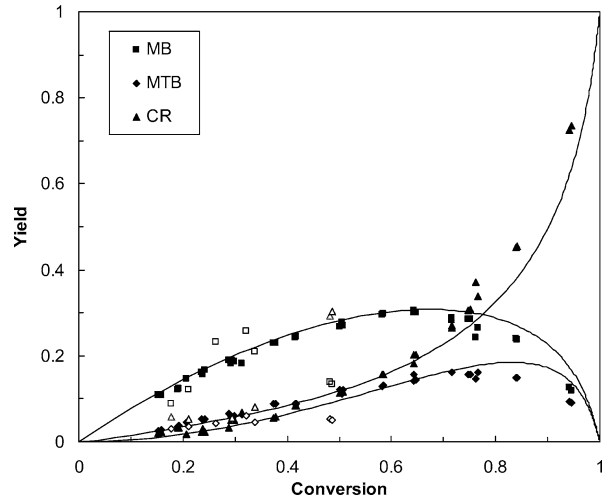

Fig. 8. Yield of monobranched, multibranched, and cracked alkanes in the hydroconversion of nonane on Pt/H-Y at 230 °C as a function of the total conversion (open symbols, pure nonane in the vapor phase; closed symbols, nonane in mixture with heptane in the liquid phase; lines, model values).

the presence of which certainly influences the adsorption behavior.

The theoretical explanation of the inversion of adsorption selectivity is given by the concept of size entropy [18,19]. According to this theory, the adsorption selectivity in pores of molecular size depends not only on the low coverage Henry constants of the competing compounds but also on the molecular sizes. At low partial pressures, when the adsorbed molecules show only weak mutual interaction, the relative amounts adsorbed are proportional to the ratio of Henry constants. With increasing pressure and thus increasing degree of pore filling, molecular size effects become important. Significant negative entropy contributions must be invested to completely fill the empty spaces in the pores. As smaller molecules pack more easily in constrained spaces, they will finally replace the bigger ones at high pressure.

The H-Y zeolite used in this work is not used commercially in *n*-alkane hydroisomerization, because it has inferior activity compared, e.g., to mordenite. It remains to be investigated whether the currently observed adsorption selectivity reversal can also be realized in other zeolites such as mordenite.

The difference in adsorption behavior between liquid- and vapor-phase conditions has important consequences for the isomer yield and product distribution. In Fig. 7, the yield of iso-alkanes and cracked alkanes in the hydroconversion of heptane on Pt/H-Y at 230 °C is plotted as a function of the conversion, for the experiments with pure heptane in the vapor phase and heptane in its mixture with nonane in the vapor phase. In accordance to the reaction scheme Eq. (4), monobranched alkanes are already formed at low conversions and subsequently isomerized in to multibranched alkanes. The maximum yield of monobranched alkanes is about 0.55. Multibranched iso-heptanes are easily cracked, explaining their lower yield. Similar conversion profiles are obtained for the pure component as for the heptane/nonane mixture under vapor-phase conditions (Fig. 7). A comparable picture is obtained with pure nonane in the vapor phase, although the isomer yield is lower due to the higher sensitivity of the nonane isomers to cracking reactions (Fig. 8). Hydroconversion of nonane under liquid-phase conditions follows the same pattern, but at the highest experimental conversion, a sudden drop in isomer yield is observed. In the hydrocracking of alkanes, hydrogen is consumed. Due to the lower hydrogen to hydrocarbon ratio under liquid-phase conditions (0.5 compared to 13 in vapor phase), depletion of dissolved hydrogen in the liquid mixture occurs at higher conversion levels, when cracking occurs, leading to a deviation from the ideal hydroconversion scheme.

Fig. 9 shows the theoretical yield curves for the hydroconversion of an equimolar heptane/nonane mixture under vapor- and liquid-phase conditions. These curves were generated using the parameters obtained from the liquid- and vapor-phase catalytic experiments and show the sum of heptane and nonane isomers or cracked products as a function of the average mixture conversion. At high pressure in the liquid phase, a significantly higher yield of isomers is obtained as compared to vapor-phase conditions, and cracking becomes important only at relatively high average conversions. In the vapor phase, nonane is selectively adsorbed and converted almost completely into (weakly adsorbing) cracked products before adsorption and conversion of heptane starts. Consequently, light cracking products are already formed at low average conversions. In the liquid phase contrarily, heptane and nonane are adsorbed simultaneously from the lowest level of conversion on; thus, isomers of both heptane and nonane are formed at low contact times. Cracking of both components starts at relatively high average conversion levels, when they are already transformed into iso-alkanes. Operating at high pressure in the liquid phase thus allows higher

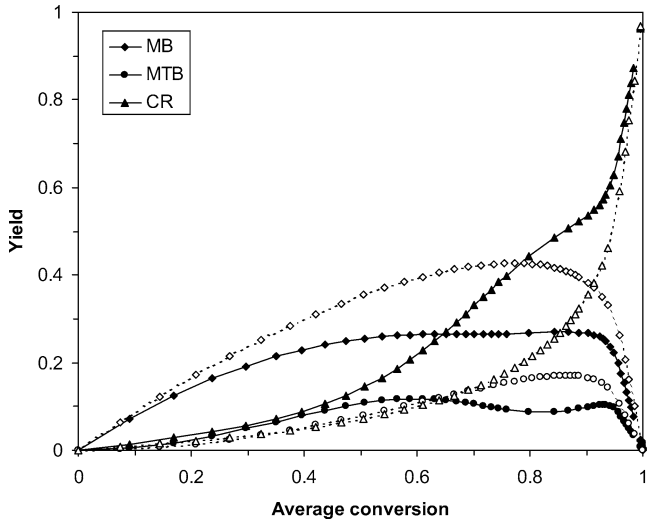

Fig. 9. Theoretical yield of monobranched, multibranched, and cracked alkanes in the hydroconversion of an equimolar heptane/nonane mixture on Pt/H-Y (open symbols, liquid phase; closed symbols, vapor phase).

isomerate yields to be obtained at lower reactor severities.

5. Conclusions

In the hydroconversion of alkane mixtures on Pt/HY, hydrocarbon partial pressure has a large influence on the observed reactivities of individual components of a mixture. While at low hydrocarbon partial pressure, the heaviest compounds of the mixture are converted much faster than the light compounds, almost no differences in apparent reactivity occur in the liquid phase, at high pressure. Analysis of the liquid-phase mixture conversion data using an appropriate kinetic model shows a reversion of the adsorption selectivity. Under liquid-phase conditions, the concentration of the shortest alkane in the supercages of the Pt/H-Y zeolite is higher than that of the longest alkane, which is the opposite to that observed in low-pressure vapor-phase conditions. Configurational-bias Monte Carlo simulations show that for the adsorption of an equimolar heptane/nonane mixture on NaY, nonane molecules are expelled in favor of the smaller heptane molecules at high pressure as a result of a size entropy effect. This preferential adsorption of the shortest alkane explains its enhanced observed reactivity under liquid-phase reaction conditions at 100 bar.

The results from this work suggest that in addition to a correct choice of a catalyst with a pore system of appropriate molecular dimensions, the possibility of adjusting the operating conditions (pressure, temperature) offers unheard opportunities to tune the relative reactivities of individual compounds. Adjustment of the reactor pressure allows varying from a regime in which the heaviest molecules are primarily converted to conditions where the lightest molecules are selectively converted into their products.

Acknowledgments

This research was financially supported by FWO Vlaanderen (G.0127.99). J. Denayer is grateful to the F.W.O.-Vlaanderen, for a fellowship as postdoctoral researcher. W.H. acknowledges the Flemish I.W.T. for a PhD fellowship. S.C., R.K., and B.S. thank the Netherlands Research Council for Chemical Sciences (CW) for partial support and the European Commission for a Marie Curie Individual Research Fellowship (to S.C.). The CHIS and COK teams participate in the IAP-PAI programme on Supramolecular Chemistry and Catalysis, sponsored by the Belgian government. The team from K.U. Leuven acknowledges the Flemish Government for a G.O.A. grant.

References

[1] H. Dauns, J. Weitkamp, Chem.-Ing.-Techn. 11 (1986) 900.
[2] J.F.M. Denayer, G.V. Baron, J.A. Martens, Phys. Chem. Chem. Phys. 2 (2000) 1007.
[3] I.E. Maxwell, W.J.H. Stork, Stud. Surf. Sci. Catal. 137 (2001) 747.
[4] R.A. Flinn, O.A. Larson, H. Beuther, Ind. Eng. Chem. 52 (1960) 153.
[5] G.F. Froment, Catal. Today 1 (1987) 455.
[6] H.L. Coonradt, W.E. Garwood, I&EC Process Design Dev. 1 (1964) 38.
[7] J.A. Martens, P.A. Jacobs, J. Weitkamp, Appl. Catal. 20 (1986) 239.
[8] J.A. Martens, P.A. Jacobs, J. Weitkamp, Appl. Catal. 20 (1986) 283.
[9] W.O. Haag, R.M. Lago, P.B. Weisz, Faraday Disc. 72 (1982) 317.
[10] J. Wei, J. Catal. 76 (1982) 433.
[11] K. Beschmann, S. Fuchs, L. Riekert, Zeolites 10 (1990) 798.
[12] M. Guisnet, Catal. Today 1 (1987) 415.
[13] M. Tromp, J.A. van Bokhoven, M.T. Garriga Oostenbrink, J.H. Bitter, K.P. de Jong, J. Catal. 190 (2) (2000) 209.
[14] F.J.M.M. de Gauw, J. van Grondelle, R.A. van Santen, J. Catal. 204 (1) (2001) 53.
[15] J.F.M. Denayer, B. De Jonckheere, M. Hloch, G.B. Marin, G. Vanbutsele, J.A. Martens, G.V. Baron, J. Catal. 210 (2002) 445.
[16] J.F.M. Denayer, A. Bouyermaouen, G.V. Baron, Ind. Eng. Chem. Res. 37 (1998) 3691.
[17] J. Talbot, AIChE J. 43 (1997) 2471.
[18] R. Krishna, B. Smit, S. Calero, Chem. Soc. Rev. 31 (2002) 185.
[19] S. Calero, B. Smit, R. Krishna, PCCP 3 (2001) 4390.
[20] S. Calero, B. Smit, R. Krishna, J. Catal. 202 (2001) 395.
[21] W. Huybrechts, J. Mijoin, P.A. Jacobs, J.A. Martens, Appl. Catal. A, in press.
[22] J.F.M. Denayer, G.V. Baron, P.A. Jacobs, J.A. Martens, J. Phys. Chem. B 102 (1998) 307.
[23] G.G. Martens, G.B. Marin, AIChE J. 47 (2001) 1607.
[24] D. Frenkel, B. Smit, Understanding Molecular Simulations: From Algorithms to Applications, 2nd ed., Academic Press, San Diego, CA, 2002.
[25] D. Frenkel, G.C.A.M Mooij, B. Smit, J. Phys. Condens. Matter 4 (1992) 3053.
[26] K. Esselink, L.D.J.C. Loyens, Phys. Rev. E 51 (1995) 1560.
[27] J.P. Ryckaert, A. Bellemans, Faraday Discuss. Chem. Soc. 66 (1978) 95.
[28] A.G. Bezus, A.V. Kiselev, A.A. Lopatkin, P.Q. Du, J. Chem. Soc. Faraday Trans. 2 74 (1978) 367.
[29] A.V. Kiselev, A.A. Lopatkin, A.A. Shulga, Zeolites 5 (1985) 261.
[30] W.H. Baur, Am. Mineral. 49 (1964) 697.
[31] T.J.H. Vlugt, R. Krishna, B. Smit, J. Phys. Chem. B 103 (1999) 1102.
[32] E. Beerdsen, B. Smit, S. Calero, J. Phys. Chem. B 106 (2002) 10659.